

Stability of very-high pressure arc discharges against perturbations of the electron temperature

M. S. Benilov and U. Hechtfisher

Citation: *J. Appl. Phys.* **111**, 073305 (2012); doi: 10.1063/1.3702469

View online: <http://dx.doi.org/10.1063/1.3702469>

View Table of Contents: <http://jap.aip.org/resource/1/JAPIAU/v111/i7>

Published by the [American Institute of Physics](#).

Related Articles

Modeling of switching delay in gas-insulated trigatron spark gaps

J. Appl. Phys. **111**, 053306 (2012)

Triggering, guiding and deviation of long air spark discharges with femtosecond laser filament

AIP Advances **2**, 012151 (2012)

Three-dimensional model and simulation of vacuum arcs under axial magnetic fields

Phys. Plasmas **19**, 013507 (2012)

Spark discharge formation in an inhomogeneous electric field under conditions of runaway electron generation

J. Appl. Phys. **111**, 023304 (2012)

Analysis on the spectra and synchronous radiated electric field observation of cloud-to-ground lightning discharge plasma

Phys. Plasmas **18**, 113506 (2011)

Additional information on *J. Appl. Phys.*

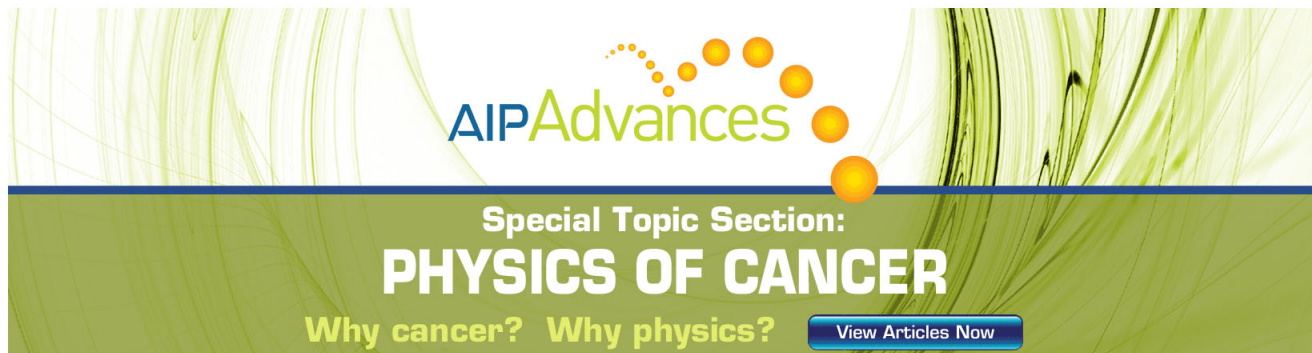
Journal Homepage: <http://jap.aip.org/>

Journal Information: http://jap.aip.org/about/about_the_journal

Top downloads: http://jap.aip.org/features/most_downloaded

Information for Authors: <http://jap.aip.org/authors>

ADVERTISEMENT



AIP Advances

Special Topic Section:
PHYSICS OF CANCER

Why cancer? Why physics? [View Articles Now](#)

Stability of very-high pressure arc discharges against perturbations of the electron temperature

M. S. Benilov¹ and U. Hechtfisher²

¹*Departamento de Física, Ciências Exactas e Engenharia, Universidade da Madeira, Largo do Município, Funchal 9000, Portugal*

²*Philips Lighting, BU Automotive Lamps, Technology, Philipsstraße 8, Aachen 52068, Germany*

(Received 12 January 2012; accepted 7 March 2012; published online 13 April 2012; publisher error corrected 19 April 2012)

We study the stability of the energy balance of the electron gas in very high-pressure plasmas against longitudinal perturbations, using a local dispersion analysis. After deriving a dispersion equation, we apply the model to a very high-pressure (100 bar) xenon plasma and find instability for electron temperatures, T_e , in a window between 2400 K and 5500-7000 K, depending on the current density (10^6 – 10^8 A/m²). The instability can be traced back to the Joule heating of the electron gas being a growing function of T_e , which is due to a rising dependence of the electron-atom collision frequency on T_e . We then analyze the T_e range occurring in very high-pressure xenon lamps and conclude that only the near-anode region exhibits T_e sufficiently low for this instability to occur. Indeed, previous experiments have revealed that such lamps develop, under certain conditions, voltage oscillations accompanied by electromagnetic interference, and this instability has been pinned down to the plasma-anode interaction. A relation between the mechanisms of the considered instability and multiple anodic attachments of high-pressure arcs is discussed. © 2012 American Institute of Physics. [<http://dx.doi.org/10.1063/1.3702469>]

I. INTRODUCTION

Very high-pressure xenon arc lamps develop, under certain conditions, voltage oscillations accompanied by electromagnetic interference (EMI).¹⁻⁵ The question arises in which region of the discharge the instability responsible for these oscillations develops and what its mechanism is.

This question was considered in Ref. 1. The near-cathode region was ruled out on the grounds that the measurements did not show any influence of the mode of operation of the cathode. The near-anode region was ruled out as well, one of the reasons being that all attempts of modeling an anodic sheath instability led to the conclusion that the anodic sheath is stable under the conditions considered. Accordingly, the conclusion was that the instability develops in the plasma column. This conclusion was supported by a local dispersion analysis, which revealed the potential presence of an instability of the energy balance of the electron gas in the plasma column. This instability has been described previously (e.g., Ref. 6, p. 61) and originates in the variations of heating of the electron gas by the electric field occurring faster than the variations of cooling by collisions with heavy particles.

However, subsequent experimental investigations of the voltage oscillations which can occur in xenon arc lamps operated at very high pressures have pinned down the instability to the near-anode region rather than to the plasma column.³⁻⁵ In particular, it was found that EMI is correlated with the temperature of the surface of the anode and the type of arc attachment to the anode. Therefore, the theoretical mechanism of instability leading to voltage oscillations under conditions of very high-pressure arc lamps must be revisited. A related topic of considerable interest is a potential relation between this mechanism and that of multiple

attachments of high-pressure arcs to the anodes, e.g., Refs. 7–13.

These tasks are dealt with in the present work. The outline of the paper is as follows: A local dispersion analysis of the stability of the energy balance of the electron gas in a quasi-neutral plasma is briefly described in Sec. II and applied to a Xe plasma in Sec. III. The results are applied to investigate the stability of very high-pressure Xe lamps in Sec. IV. A relation between the mechanisms of the considered instability and multiple anodic attachments of high-pressure arcs is discussed in Sec. V. Conclusions are summarized in Sec. VI.

II. DISPERSION ANALYSIS

The instability of the energy balance of the electron gas in a quasi-neutral plasma and the procedure of its dispersion analysis have been described in the literature (page 61 of Ref. 6). Following Ref. 1, we start with the equations of conservation of number and energy of electrons in a collisional quasi-neutral plasma with a Maxwellian electron energy distribution. These equations can be written in the form (e.g., p. 428 of Ref. 14)

$$\frac{\partial n_e}{\partial t} + \nabla \cdot \left(n_e \mathbf{v} - \frac{\mathbf{j}_e}{e} \right) = w, \quad (1)$$

$$\begin{aligned} \frac{D}{Dt} \left[n_e \left(\frac{3}{2} kT_e + E_i \right) \right] + n_e \left(\frac{5}{2} kT_e + E_i \right) \nabla \cdot \mathbf{v} \\ + \nabla \cdot \left(\mathbf{q}_e - E_i \frac{\mathbf{j}_e}{e} \right) = \mathbf{j}_e \cdot \mathbf{E} - w_{elast} - w_{rad}. \end{aligned} \quad (2)$$

Here and further indices a , i , and e are attributed to the neutral particles, ions, and electrons, respectively; n_x is the

number density of a species α ($\alpha = a, i, e$); T_e is the electron temperature; \mathbf{j}_e is the density of the electric current transported by the electrons; w is the net rate of production of pairs ion-electron in volume reactions; \mathbf{v} is the mean mass velocity of the plasma; $D/Dt = \partial/\partial t + \mathbf{v} \cdot \nabla$ is the material derivative; E_i is the ionization energy; \mathbf{q}_e is the density of electron heat flux; \mathbf{E} is the electric field; and w_{elast} and w_{rad} are the rates per unit volume at which energy is lost by the electron gas as a result of elastic collisions with heavy particles and, respectively, radiation.

A conventional expression describing ionization and recombination in monoatomic gases reads

$$w = k_i n_a n_e - k_r n_e^3, \quad (3)$$

where the rate coefficients k_i and k_r are functions of the electron temperature: $k_i = k_i(T_e)$, $k_r = k_r(T_e)$.

The electric field in the Joule heating term on the rhs of Eq. (2) will be eliminated with the use of Ohm's law, $\mathbf{j}_e = en_e \mu_e \mathbf{E}$, where μ_e is the mobility of electrons.

The rate of electron energy loss in elastic collisions with heavy particles is (e.g., page 428 in Ref. 14)

$$w_{elast} = n_e \bar{v}_{eh} \frac{2m_e}{m_a} \frac{3}{2} k(T_e - T_h). \quad (4)$$

Here, T_h is the temperature of the heavy particles (atoms and ions) and \bar{v}_{eh} is the average frequency of momentum transfer in collisions of electrons with the heavy particles defined by the formula

$$\bar{v}_{eh} = \frac{4}{3} \bar{C}_e \left(n_a \bar{Q}_{ea}^{(1,1)} + n_i \bar{Q}_{ei}^{(1,1)} \right), \quad (5)$$

where $\bar{C}_e = (8kT_e/\pi m_e)^{1/2}$ is the electron mean thermal speed and $\bar{Q}_{ea}^{(1,1)}$ and $\bar{Q}_{ei}^{(1,1)}$ are average cross sections for momentum transfer in collisions between electrons and atoms and electrons and ions, respectively.

Making use of Eq. (1), Eq. (2) may be re-written as

$$n_e \frac{3}{2} k \frac{DT_e}{Dt} + \frac{3}{2} k T_e \nabla \cdot \frac{\mathbf{j}_e}{e} + n_e k T_e \nabla \cdot \mathbf{v} + \nabla \cdot \mathbf{q}_e = n_e \frac{3}{2} k H. \quad (6)$$

Here, the auxiliary quantity H abbreviates

$$H = \frac{2j_e^2}{3ken_e^2 \mu_e} - \frac{2e}{m_a \mu_e^{[1]}} (T_e - T_h) - \frac{2}{3k} \frac{w}{n_e} \left(\frac{3}{2} k T_e + E_i \right) - \frac{2}{3k} \frac{w_{rad}}{n_e}, \quad (7)$$

where $\mu_e^{[1]} = e/m_e \bar{v}_{eh}$ may be interpreted as an approximate value of the mobility of electrons. (In the accurate kinetic theory, $\mu_e^{[1]}$ represents the value given by the first approximation in the expansion in Sonine polynomials in the Chapman-Enskog formalism.)

The linear stability theory is a conventional tool for investigation of the onset of instability. (Of course, a nonlinear analysis is required to study voltage spikes observed in Refs. 1, 5, which represent a result of development of the

considered instability and cannot be described under the assumption of small perturbations.) Following the usual procedure (e.g., page 217 in Ref. 15), we represent the time-dependent quantities as superpositions of the corresponding steady-state value and a small perturbation with an exponential time dependence,

$$n_e(t) = n_{e0} + e^{\lambda t} n_{e1}, \quad T_e(t) = T_{e0} + e^{\lambda t} T_{e1}, \quad (8)$$

where λ is the increment (rate of growth) of perturbations, which is the quantity to be found. Substituting the expressions in Eq. (8) into Eqs. (1) and (6), expanding in n_{e1} and T_{e1} and retaining linear terms, one arrives at equations for n_{e1} and T_{e1} .

Similarly to Ref. 1, this work is limited to a local dispersion analysis, which amounts to neglecting spatial gradients in the above-mentioned linear equations for n_{e1} and T_{e1} . It is well known that transversal perturbations, i.e., those which vary in a direction perpendicular to the discharge current and result in contraction of the discharge current and appearance of filaments, perturb the discharge current, but the electric field remains unaffected, whereas longitudinal perturbations, i.e., those which vary in a direction along the discharge current and result in appearance of striations or domains, perturb the electric field, but the discharge current remains unaffected, e.g., pages 60 and 61 in Ref. 6 or pages 219 and 221 in Ref. 15. Since oscillations of the discharge voltage observed in Refs. 1, 5 mean that the electric field is perturbed, it is appropriate here to consider longitudinal perturbations. Therefore, the current density is treated as a given quantity not subject to perturbations. The contribution of the ion current is neglected, i.e., the (net) current density j is assumed to be equal to the electron current density j_e . Variations of the number density of neutral atoms and of the temperature of atoms and ions are neglected as well.

In the above framework, the quantities w and H may be treated as functions of n_e and T_e : $w = w(n_e, T_e)$, $H = H(n_e, T_e)$, and the above-mentioned linear equations for perturbations assume the form

$$\lambda n_1 = \frac{\partial w}{\partial n_e} n_{e1} + \frac{\partial w}{\partial T_e} T_{e1}, \quad (9)$$

$$\lambda T_{e1} = \frac{\partial H}{\partial n_e} n_{e1} + \frac{\partial H}{\partial T_e} T_{e1}. \quad (10)$$

(The derivatives are evaluated at $n_e = n_{e0}$, $T_e = T_{e0}$.) This system of linear algebraic equations for n_{e1} and T_{e1} admits nontrivial solutions, provided that its determinant vanishes. The latter condition represents a dispersion equation governing the increment λ . A solution to this (quadratic) equation reads

$$\lambda_{1,2} = \frac{b}{2} \pm \sqrt{\frac{b^2}{4} - c}, \quad (11)$$

where

$$b = \frac{\partial w}{\partial n_e} + \frac{\partial H}{\partial T_e}, \quad c = \frac{\partial w}{\partial n_e} \frac{\partial H}{\partial T_e} - \frac{\partial H}{\partial n_e} \frac{\partial w}{\partial T_e}. \quad (12)$$

The real part of the solution in Eq. (11) with the sign plus (λ_1) is larger than or equal to the real part of the solution in Eq. (11) with the sign minus (λ_2). Therefore, it is sufficient to evaluate the root λ_1 : $\text{Re } \lambda_1 > 0$ implies instability, with $(\text{Re } \lambda_1)^{-1}$ being a characteristic time of its development, and $\text{Re } \lambda_1 < 0$ implies stability, with $-(\text{Re } \lambda_1)^{-1}$ being a characteristic time of decay of perturbations.

III. INCREMENT OF PERTURBATIONS IN A VERY HIGH-PRESSURE Xe PLASMA

From Sec. II, we now have a model giving the increment of perturbations of electron temperature in a uniform high-pressure plasma. The input parameters include those characterizing the steady state in which stability is investigated: the electron and heavy-particle temperatures T_e and T_h , the electron density n_e , and the neutral-atom density n_a , or, alternatively, the plasma pressure p . (The index 0 referring to unperturbed plasma parameters is dropped for brevity here and further.) Another control parameter is the current density, j , which is needed for evaluation of derivatives of the function $H(n_e, T_e)$.

Results reported in this work refer to a very high-pressure Xe plasma. The transport and kinetic coefficients of this plasma and the radiation energy losses have been evaluated in the same way as in Ref. 16. The derivatives $\partial H/\partial n_e$ and $\partial w/\partial T_e$, $\partial H/\partial T_e$ have been found by means of numerical differentiation, the steps being $10^{-3} n_e$ and $10^{-3} T_e$, respectively. An important particular case is that where the steady states being considered are local thermodynamic equilibrium (LTE) ones, i.e., both the ionization and thermal equilibrium hold in these states: $n_e = n_s$, $T_e = T_h$ (n_s is the electron density evaluated by means of the Saha equation). It is sufficient to specify just three control parameters in this case: T_e , p , and j . We assume a pressure of $p = 100$ bar and a current density, j , in the range 10^6 – 10^8 A/m²: parameters that are typical for very high-pressure xenon arc lamps, for example, for those studied experimentally in Ref. 5. This section is concerned with finding values of electron temperature at which the instability can develop; the question of whether these values do occur inside very high-pressure xenon arc lamps is treated in Sec. IV.

The real part of the increment of perturbations of the LTE high-pressure Xe plasma is shown in Fig. 1. One can see that there is a range of T_e where $\text{Re } \lambda_1$ is positive. We will refer to this range as the window of instability. $\text{Re } \lambda_1$ is quite high inside this window, of the order of 10 ns^{-1} or higher. Outside this window, $\text{Re } \lambda_1 < 0$; however, values of $|\text{Re } \lambda_1|$ are substantially smaller than those inside the window (typically of the order of $1 \mu\text{s}^{-1}$ or smaller) and their sign cannot be seen from Fig. 1. The lower and upper boundaries of the instability window, $T_e^{(inst)}$ and $T_e^{(stab)}$, are shown in Table I. The lower boundary is virtually independent of j and is close to 2400 K for all values of j . The upper boundary slowly increases with increasing j . The imaginary part of λ_1 turns out to be negligible except in a narrow range of T_e around the upper boundary of the instability window.

Also shown in Table I are the lower and upper boundaries of the instability window for a plasma in thermal

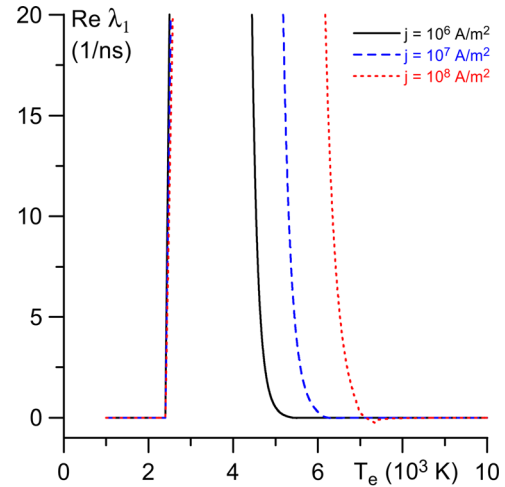


FIG. 1. Real part of increment of perturbations of LTE high-pressure Xe plasma. $p = 100$ bar.

non-equilibrium, $T_e > T_h$, but still in ionization equilibrium, $n_e = n_s$, for two values of the temperature difference $\Delta T = T_e - T_h$ ($\Delta T = 1000$ K, 3000 K), and for a plasma in ionization non-equilibrium, $n_e > n_s$, but still in thermal equilibrium, $T_e = T_h$, for $n_e/n_s = 2$. One can see that the instability window depends little on what is assumed for ΔT or n_e/n_s .

In order to elucidate the meaning of these results, let us consider the coefficients b and c defined by Eqs. (12). The coefficient c turned out positive in all the calculations performed in this work. Therefore, the sign of $\text{Re } \lambda_1$ is determined by the sign of b , irrespective of λ_1 being real or complex. It follows that the change of sign of $\text{Re } \lambda_1$ seen in Fig. 1 is associated with the change of sign of b : b is positive inside the instability window and negative outside. At a state where the change of stability occurs, $b = 0$ and the increment λ_1 is imaginary: $\lambda_1 = i\sqrt{c}$; in other words, neutrally stable perturbations are oscillatory rather than stationary. Therefore, the fact that complex values of λ_1 were detected near the upper boundary of the instability window, but not near the lower boundary, means that the vicinity of the lower boundary in which the perturbations are oscillatory is narrower than 1 K (this was the step in T_e used in the calculations).

Furthermore, it was found that $b^2 \gg c$ in all the calculations except in the vicinity of the upper boundary of the instability window. In this case, one can simplify expression

TABLE I. The lower and upper boundaries of the instability window, $T_e^{(inst)}$ and $T_e^{(stab)}$. Xe plasma, $p = 100$ bar. ΔT : difference between electron and heavy-particle temperatures. n_s : electron density as evaluated by means of the Saha equation.

j (A/m ²)	ΔT (K)	n_e/n_s	$T_e^{(inst)}$ (K)	$T_e^{(stab)}$ (K)
10^6	0	1	2400	5436
10^7	0	1	2400	6251
10^8	0	1	2400	7144
10^7	1000	1	2400	6204
10^7	3000	1	< 3100	6082
10^7	0	2	2400	5912

(11) and find $\lambda_1 \approx b$ and $\lambda_2 \approx c/b$ if $b > 0$ and $\lambda_1 \approx c/b$ and $\lambda_2 \approx b$ if $b < 0$. The physical sense is clear: one of the perturbation modes is fast and the other is slow; their increments equal b and c/b , respectively; if $b > 0$, both modes are growing in time and the rate of growth of perturbations is governed by the fast mode; and if $b < 0$, both modes are decaying and the rate of decay of perturbations is governed by the slow mode. This explains the difference in orders of magnitude of $\text{Re } \lambda_1$ inside and outside the instability window, seen in Fig. 1, and also the fact that the vicinities of the boundaries of the instability window where λ_1 is complex are so narrow.

It was also found in the calculations that $|\partial H/\partial T_e| \gg |\partial w/\partial n_e|$: the time of relaxation of the electron temperature is much shorter than the time of relaxation of the electron density, similarly to what happens in glow discharges (Ref. 6, p. 60). Using this inequality and Eq. (12), one can express the increments of the fast and slow perturbation modes as, respectively,

$$b \approx \frac{\partial H}{\partial T_e}, \quad \frac{c}{b} \approx \frac{\partial w}{\partial n_e} - \frac{\partial w}{\partial T_e} \frac{\partial H}{\partial n_e} \left(\frac{\partial H}{\partial T_e} \right)^{-1}. \quad (13)$$

The first expression in Eq. (13) represents a solution of Eq. (10), with the first term on the rhs of the latter equation being dropped. One can conclude that the instability seen in Fig. 1 indeed represents an instability of the energy balance of the electron gas and that the electron density remains frozen during the development of this instability, similarly to how it happens in glow discharges (Ref. 6, p. 60).

In accordance with the above, the criterion of instability reads $\partial H/\partial T_e > 0$ or, equivalently,

$$r_1 + r_2 + r_3 + r_4 > 0, \quad (14)$$

where r_1, r_2, r_3 , and r_4 are derivatives with respect to T_e of the corresponding terms on the right-hand side of Eq. (7),

$$r_1 = \frac{2j_e^2}{3ken_e^2} \frac{\partial}{\partial T_e} \left(\frac{1}{\mu_e} \right), \quad r_2 = -\frac{2e}{m_a} \frac{\partial}{\partial T_e} \left(\frac{T_e - T_h}{\mu_e^{[1]}} \right), \quad (15)$$

$$r_3 = -\frac{2}{3kn_e} \frac{\partial}{\partial T_e} \left[w \left(\frac{3}{2} kT_e + E_i \right) \right], \quad r_4 = -\frac{2}{3kn_e} \frac{\partial w_{\text{rad}}}{\partial T_e}. \quad (16)$$

Obviously, these terms represent contributions to the increment or instability of, respectively, Joule heating of the electron gas, losses of electron energy in elastic collisions with heavy particles, losses of electron energy due to ionization, and losses of electron energy due to excitation of neutral atoms with subsequent emission of a photon.

Let us analyze the effect of these different terms r_1, r_2, r_3 , and r_4 on b (and thus on the sign of the increment $\text{Re } \lambda_1$). If the steady state being considered is that of thermal equilibrium, $T_e = T_h$, then Eq. (15) yields $r_2 = -2e/m_a \mu_e^{[1]}$ so that r_2 is negative. In fact, r_2 was found to be negative in all the calculations performed in this work and also in those with $T_e \neq T_h$. With increase of T_e , $k_i(T_e)$ grows, while $k_r(T_e)$ decreases. Then it follows, from Eq. (3), that $\partial w/\partial T_e > 0$,

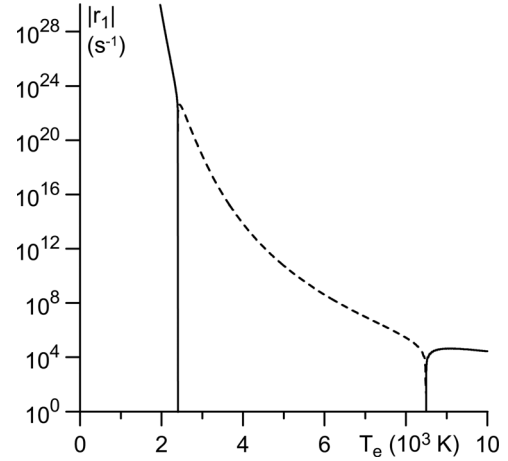


FIG. 2. Contribution of Joule heating to the increment of instability of electron energy balance in high-pressure LTE Xe plasma. $p = 100$ bar, $j = 10^7$ A/m². Solid: negative values of r_1 . Dashed: positive values of r_1 .

and it follows from the first equation in Eq. (16) that $r_3 < 0$. The radiation losses increase with increase of T_e , hence $r_4 < 0$.

Thus, the terms r_2, r_3 , and r_4 on the left-hand side of the inequality in Eq. (14) are negative, and the only term that may be positive is r_1 . This term is illustrated by Fig. 2. r_1 is positive inside the instability window, as it should have been expected, and also in a certain range of T_e above the window.

The contributions of the different terms to the increment are illustrated by Fig. 3. For completeness, all the terms constituting the quantity b are shown, including the term $r_5 = \partial w/\partial n_e$ from the (original) first equation in Eq. (12). Each term is normalized by $|r_1| + \dots + |r_5|$. For $T_e < 2400$ K, r_1 is negative and much larger than all the other terms. For $2400 \text{ K} < T_e \lesssim 6000$ K, r_1 becomes positive and remains dominating. For T_e exceeding approximately 6000 K, the terms r_2 and r_3 come into play and the contribution of r_1 starts decreasing. While the term r_2 reaches a value which does not exceed approximately 30% and then starts decreasing, the term r_3 continues to increase and, for $T_e \gtrsim 7000$ K, becomes dominating. The term r_4 is negligible for all T_e . The

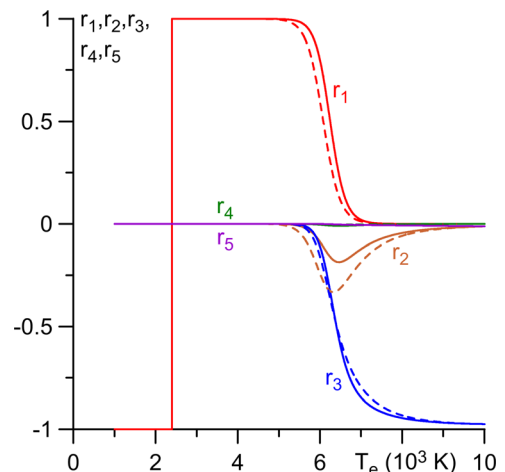


FIG. 3. Normalized contributions of different mechanisms to the increment of instability of electron energy balance in high-pressure Xe plasma. $p = 100$ bar, $j = 10^7$ A/m². Solid: $T_h = T_{e0}$. Dashed: $T_h = T_{e0} - 3000$ K.

term r_5 is negligible as well, in agreement to what was said above.

Thus, the most important mechanisms governing the (in)stability under the conditions of the very high-pressure arc discharges considered here are Joule heating of the electron gas (term r_1) and losses of electron energy due to ionization (r_3) and elastic collisions with heavy particles (r_2). Joule heating of the electron gas can produce both stabilizing ($r_1 < 0$) and destabilizing ($r_1 > 0$) effects; losses of electron energy can play only a stabilizing role (r_2 and $r_3 < 0$). With increasing T_e , the instability appears when the effect of Joule heating switches from stabilizing to destabilizing and disappears when the destabilizing effect of Joule heating is overcome by the stabilizing effect of losses of electron energy, in the first place, due to ionization.

According to the first equation in Eq. (15), switching of the role played by the Joule heating from stabilization ($r_1 < 0$) to destabilization ($r_1 > 0$) is due to a non-monotonic dependence of electron mobility on T_e . In order to illustrate this dependence, let us rewrite the first expression in Eq. (15) as

$$r_1 = \frac{2 J_e^2 m_e}{3k e^2 n_e^2} \frac{\partial}{\partial T_e} \left(\frac{\bar{v}_{eh}}{\zeta_e} \right), \quad (17)$$

where $\zeta_e = \mu_e/\mu_e^{[1]}$ is a kinetic coefficient of order unity and \bar{v}_{eh} is, as before, the average frequency of momentum transfer in collisions of electrons with the heavy particles. The dependence of \bar{v}_{eh} on T_e can be derived from Eq. (5). The average electron-ion elastic-scattering cross section $\bar{Q}_{ei}^{(1,1)}$ is proportional to T_e^{-2} , apart from a weak dependence on T_e through the Coulomb logarithm. Hence, at high T_e , where the charged particle density is high enough and the Coulomb collisions prevail, $n_a \bar{Q}_{ea}^{(1,1)} \ll n_i \bar{Q}_{ei}^{(1,1)}$, \bar{v}_{eh} is approximately proportional to $T_e^{-3/2}$. It follows from Eq. (17) that $r_1 < 0$, i.e., Joule heating plays a stabilizing role. This means that the instability may occur only at low T_e , where the charged particle density is low enough so that $n_a \bar{Q}_{ea}^{(1,1)} \gtrsim n_i \bar{Q}_{ei}^{(1,1)}$, and only if the electron-atom collision frequency $\bar{v}_{ea} = \frac{4}{3} \bar{C}_e n_a \bar{Q}_{ea}^{(1,1)}$ increases with T_e . Note that, since variations of the number density of neutral atoms are neglected in the present analysis, the latter statement refers to the dependence of \bar{v}_{ea} on T_e at fixed n_a or, equivalently, to the dependence on T_e of the ratio $\bar{v}_{ea}/n_a = \frac{4}{3} \bar{C}_e \bar{Q}_{ea}^{(1,1)}$.

The latter dependence evaluated for the case of Xe atoms is depicted in Fig. 4. Also shown are the average collision cross section $\bar{Q}_{ea}^{(1,1)}$ and the kinetic coefficient $\zeta_{ea} = \mu_{ea}/\mu_{ea}^{[1]}$ (here, μ_{ea} is the mobility of electrons in the gas of neutral atoms and $\mu_{ea}^{[1]} = e/m_e \bar{v}_{ea}$). The vertical dashed line in this figure represents the above-described lower boundary of the instability window, $T_e = 2400$ K. One can see that the instability window opens at the minimum of the function \bar{v}_{ea}/n_a , in agreement with the above reasoning.

The non-monotonic behavior of \bar{v}_{ea} is due to the non-monotonic behavior of the cross section $\bar{Q}_{ea}^{(1,1)}$, which, in turn, is due to the Ramsauer effect. One can see that the lower boundary of the instability window is not far away from the Ramsauer minimum. (We remind that $\bar{Q}_{ea}^{(1,1)}$ is the

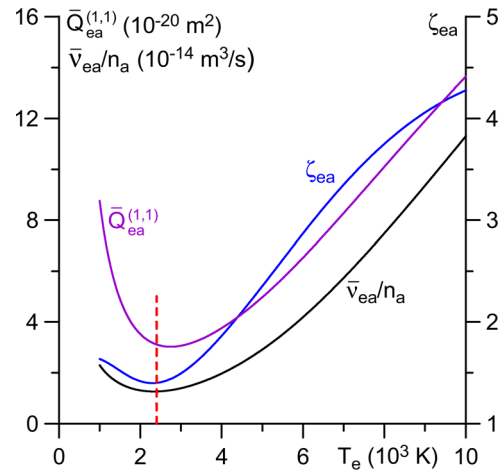


FIG. 4. Kinetic coefficients characterizing transport of electrons in the gas of Xe atoms.

average cross section for momentum transfer in collisions between electrons and xenon atoms; the Ramsauer minimum in the energy-dependent momentum-transfer cross section is positioned at approximately 0.7 eV.)

IV. APPLICATION TO VERY HIGH-PRESSURE Xe LAMPS

In order to decide whether the instability can occur in a high-pressure gas discharge lamp, one needs to check whether values of the electron temperature within the instability window can occur inside the lamp.

Simple estimates for conditions of high-pressure discharge lamps¹⁷ show that the plasma is close to LTE and the energy balance of the plasma is dominated by radiation (i.e., Joule heating in the plasma is locally compensated by radiation cooling) in the bulk plasma, which includes the arc column and near-electrode constriction zones. In such a case, the local temperature can be estimated in terms of the local current density and plasma pressure. Therefore, it is sufficient to specify just two control parameters in this case: p and j .

Results of evaluation of the increment for such conditions are shown in Fig. 5. Also shown is T_{eq} , the local

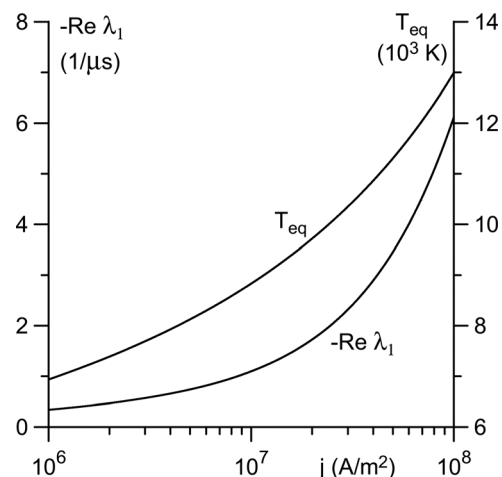


FIG. 5. Increment of perturbations in a radiation-dominated very high-pressure LTE Xe plasma. $p = 100$ bar.

temperature evaluated assuming a radiation-dominated energy balance. One can see that T_{eq} rises from about 7000 K at $j = 10^6 \text{ A/m}^2$ to about 13 000 K at 10^8 A/m^2 . Since even the lowest value (7000 K) is still above the instability window detected for these conditions in Sec. III, it is unsurprising that the increment λ_1 , which is calculated for these conditions under the assumption $T_e = T_h = T_{eq}$ (and $n_e = n_s$), possesses a negative real part for all values of j , as seen in Fig. 5. It follows that the instability cannot develop in the radiation-dominated bulk of a very high-pressure Xe arc.

In the near-electrode layers of the arc (e.g., Ref. 17), the local energy balance of the plasma is perturbed by heat conduction and the plasma is no longer dominated by radiation; the local balance of charged particles is perturbed by ambipolar diffusion, i.e., the ionization equilibrium does not hold, and the heavy-particle temperature deviates from the electron temperature. Therefore, one needs to solve differential equations involving spatial derivatives in order to find an adequate description of the near-electrode layers, namely, equations of conservation of the charged particles, electron energy, and energy of the heavy particles. Such solutions under conditions of interest for this work have been reported in Refs. 18 and 16 for the near-cathode and near-anode layers, respectively. An analysis of the modeling results¹⁸ reveals that the electron temperature in the near-cathode layer is even higher than in the bulk plasma and thus also clearly above the instability window, so that the instability cannot develop in the near-cathode layer either. For the near-anode layer, on the other hand, modeling results¹⁶ predict significantly lower values of T_e , down to about 5000 K, which lies inside the instability window predicted here. This leaves the near-anode layer as the only region in a very high-pressure Xe lamp where the instability can occur.

This conclusion agrees with the experimental investigations³⁻⁵ of voltage oscillations in very-high-pressure Xe arcs, which, as discussed in the introduction, pinned down the instability to the near-anode region. The theoretical time of development of the instability, $(\text{Re } \lambda_1)^{-1}$, which is of the order of 0.1–1 ns, conforms to the rise time of a single pulse, which was experimentally determined to be about 800 ps or shorter.¹ Since the imaginary part of the increment is negligible in nearly all the cases, the perturbations grow monotonically on the linear stage of the development of the instability and the oscillations develop on the nonlinear stage.

When focusing the present stability analysis to the near-anode layer of very high-pressure Xe lamps, some of the early premises have to be revisited. The ionization degree corresponding to $T_e^{(stab)}$ under the conditions of Table I is below 0.1%, even in the case of a current density at the anode surface as high as 10^8 A m^{-2} . Perturbations of the density, velocity, and energy of charged particles and of the electric field do not appreciably affect the neutral atoms for ionization degrees that low, which justifies the neglect of variations of the number density and temperature of neutral atoms in the analysis of Sec. II.

The deviation of parameters of the xenon plasma at a pressure of 100 bar and temperatures exceeding 2000 K from the equation of state of ideal gas, estimated by means of the

Van der Waals equation, is no more than 3%. The ideal-gas approximation is adequate under such conditions.

In order to get an idea of the time scale of relaxation of deviations from quasi-neutrality, let us estimate the time of diffusion of the electrons over a distance Δ equal to the scale of thickness of the near-anode space-charge sheath. Data in Fig. 5 of Ref. 16, which refers to a 100-bar xenon plasma as well, suggest $\Delta = 0.3 \mu\text{m}$. Setting the diffusion coefficient of electrons in the gas of neutral atoms D_{ea} equal to $4 \times 10^{-2} \text{ m}^2 \text{ s}^{-1}$ (a value for a 100-bar xenon plasma at $T_e = T_h = 5 \times 10^3 \text{ K}$), one finds $\Delta^2/D_{ea} \approx 2 \text{ ps}$. This time is substantially shorter than the time of development of the instability $(\text{Re } \lambda_1)^{-1}$. It follows that the plasma remains quasi-neutral while the instability develops, which justifies the corresponding assumption made in the analysis of Sec. II.

The treatment of Sec. II refers to spatially uniform plasmas, and its application to the near-anode layer, where gradients are considerable, is, strictly speaking, unjustified. However, this treatment still allows one to obtain a useful qualitative indication. Let us introduce the quantity

$$s = \frac{j}{en_e} \frac{1}{\text{Re } \lambda_1}. \quad (18)$$

The ratio j/en_e represents the local mean speed with which the electrons drift toward the anode surface. Hence, s has the meaning of a characteristic distance over which the electrons drift while the instability is developing. If this distance is larger than the distance to the anode surface, then there will be no instability, because the time of drift of the electron gas to the anode surface is insufficient for the instability to develop.

Representative calculated values of s are shown in Fig. 6. One can see that s is quite high (of the order of millimeters and higher) near the upper boundary of the instability window. Given that the thickness of the near-anode layer is of the order of 0.1 mm, one should conclude that the instability cannot develop at T_e near the upper boundary of the instability window. In other words, the T_e window of instability at a given position in the near-anode layer is narrower than in a uniform plasma with the same parameters.

To treat the nonuniform near-anode plasma properly, the next step should be to perform a linear stability analysis of differential equations describing the current transfer through the near-anode layer, similarly to how stability of current transfer to arc cathodes has been investigated.^{19,20} One can hope that this analysis will describe effects that remain unexplained at the present stage, in the first place, the surprising and very clean response of the instability to variations of the anode tip temperature.⁵ A further step will be to obtain a non-stationary numerical solution of the full (non-linear) equations, which will provide information on the oscillations.

It must be considered why our main conclusion about the instability occurring in the near-anode layer, being in agreement with the experimental data,³⁻⁵ contradicts Anders *et al.*¹, who concluded that the instability occurs in the arc column. The dispersion analyses conducted in this work and

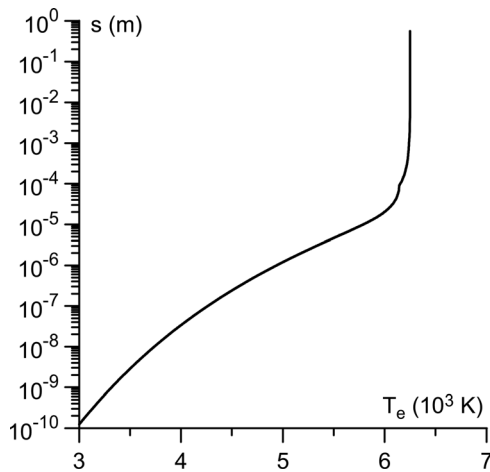


FIG. 6. Distance necessary for development of the instability in high-pressure LTE Xe plasmas. $p = 100$ bar, $j = 10^7$ A/m².

Ref. 1 are not very different. In particular, our Fig. 1 is qualitatively similar to Fig. 6 of Ref. 1, except for one aspect: while $|\text{Re } \lambda_1|$ in Fig. 6 of Ref. 1 exceeds 4 ns^{-1} for T_e below the window of instability, it is much smaller, according to the calculations of this work. This difference becomes understandable if one assumes that the increment in Fig. 6 of Ref. 1 was evaluated neglecting perturbations of the electron density, i.e., equals $\partial H / \partial T_e$ in designations of the present work. Note that this assumption, while being inconsistent with n_{eI} appearing in Ref. 1 at the last phase of the derivation of Eq. (7),¹ is consistent with the structure of the rhs of the latter equation, although the last term on the rhs is difficult to understand anyway.

Worth noting are significant differences in values of transport and kinetic coefficients between Ref. 1 and the present work. In particular, the authors¹ seem to have taken into account only direct ionization of neutral atoms, but neglected stepwise ionization, which would amount to underestimating the ionization rate by several orders of magnitude: for example, the ratio of the coefficients $k_i^{[dir]} / k_i^{(sr)}$ for $T_e = 7000$ K is about 2.8×10^{-3} . The fact that differences that significant have not produced a qualitative effect is remarkable and is likely to originate in the Arrhenius character of the processes involved.

Since the dispersion analyses conducted in this work and Ref. 1 are not very different, the difference in conclusions must originate in how results of the dispersion analysis are applied to conditions of very high-pressure Xe lamps. This is indeed the case: the authors¹ seem not to have realized that the electron temperature in the near-anode region may be significantly lower than in the arc column, as was subsequently indicated by the modeling.¹⁶

It should be stressed that possibilities of measurements of the electron temperature near anodes of high-pressure arc discharges are limited. For example, experiments showed that T_e in argon arcs at $p = 2$ bar decreases toward the anode (Fig. 9 of Ref. 21), with the T_e value at a point closest to the anode being around 8000 K; however, the spatial resolution was only of the order of $100 \mu\text{m}$. This means that such measurements cannot detect a further decrease to values of the order of 5000 K within the last $100 \mu\text{m}$ from the anode,

which is predicted by the modeling.¹⁶ In such a situation, pinning down the instability to the near-anode region³⁻⁵ together with the dispersion analysis, indicating that the instability can occur only at T_e values below those in the bulk plasma, represents an important, although inevitably indirect, experimental confirmation of the low T_e values predicted by the modeling.¹⁶

V. RELATION TO THE THEORY OF MULTIPLE ANODE ATTACHMENTS

Multiple attachments of a high-pressure arc to the anode are observed in the current range from tens of amperes to several hundred amperes, depending on the width of the electrode gap and the kind of the plasma-producing gas; see, e.g., Refs. 7–13. A theoretical analysis of the instability leading to multiple attachments was given in Refs. 7 and 11. The conclusion that is the most relevant to the present work is the following: if $d\mu_e/dT_e > 0$, which is the case if the charged particle density is high enough and electron-ion collisions prevail over electron-atom collisions, then the Joule heating produces a destabilizing effect.

This conclusion is just opposite to the conclusion of the present work: if $d\mu_e/dT_e > 0$, then it follows from Eq. (15) that $r_1 < 0$ and the Joule heating produces a stabilizing effect under the conditions of the present work, as discussed in Sect. III. Of course, this difference should have been expected: while the instability that causes multiple anode attachments consists in the development of transversal (perpendicular to the discharge current) perturbations of T_e and, therefore, develops at constant electric field, the instability that causes voltage oscillations consists in the development of longitudinal (parallel to the discharge current) perturbations of T_e and therefore develops at constant current density. The Joule heating of the electron gas in the case of a constant electric field is directly proportional to the electron mobility, while, in the case of a constant current density, it is inversely proportional to the electron mobility. Therefore, a growing dependence of the electron-atom collision frequency on the electron temperature that causes a negative derivative $d\mu_e/dT_e$ provides a stabilizing mechanism for perturbations that develop at constant electric field and a positive feedback for perturbations that develop at a constant current density.

VI. CONCLUSIONS

A local dispersion analysis of very high-pressure Xe arc plasmas has confirmed the conclusion of Ref. 1 on a possible instability against perturbations of the electron temperature parallel to the arc current. The instability has been traced back to a growing dependence of the electron-neutral collision frequency on the electron temperature. This dependence ensures that the Joule heating of the electron gas (which, in the case of a constant current density, is inversely proportional to the electron mobility) is a growing function of T_e , thus providing a positive feedback. As a manifestation of this mechanism, the value of T_e that limits the instability window in Xe from below approximately corresponds to the Ramsauer minimum of the electron-atom cross section. In principle, the instability may occur not only in Xe, but also

in other gases, for example, in Hg: there is no Ramsauer minimum in Hg and \bar{v}_{ea} for fixed n_a monotonically grows for all T_e of interest, including low values.

The conclusion of Ref. 1 that this instability develops in the arc column has not been confirmed: T_e in a very high-pressure, radiation-dominated Xe plasma is above the window of existence of the instability. The instability is not possible in the near-cathode layer either, where T_e is still higher. But according to the modeling,¹⁶ T_e goes down to quite low values (of the order of 5000 K) in the near-anode layer; then this is the only region where the instability is possible. This conclusion agrees with the experimental observations of the last decade,³⁻⁵ which pinned down the instability-caused voltage oscillations in very high-pressure Xe arcs to the near-anode region. The time of development of the instability $(\text{Re } \lambda_1)^{-1}$ conforms to the experimental rise time of a single pulse. Note that the above agreement represents an important, although inevitably indirect, confirmation of the theoretical conclusion¹⁶ that T_e in the near-anode layer of the very high-pressure arcs is quite low.

There is a similarity between the formalisms of the theory of the instability behind multiple anode attachments in high-pressure arcs and of the present theory of the instability leading to EMI. However, the mechanisms of the instabilities are different: the Joule heating effect that is stabilizing in one case is destabilizing in the other. (More precisely, it is stabilizing in the former case and destabilizing in the latter if $d\mu_e/dT_e < 0$ and the other way around if $d\mu_e/dT_e > 0$.)

The treatment of this work, being based on the local dispersion analysis, represents just the first step in the development of the theory. The next step should be to perform the linear stability analysis of differential equations describing the current transfer through the near-anode layer. One can hope that this analysis will describe, in particular, the surprising and very clean response of the instability to variations of the anode tip temperature⁵ and also will explain why this instability is not observed in very high-pressure Hg lamps. A further step will be to obtain a non-stationary

numerical solution of the full (nonlinear) equations, which will provide information on the oscillations.

ACKNOWLEDGMENTS

The work at Universidade da Madeira was supported by FCT - Fundação para a Ciência e a Tecnologia of Portugal (projects PTDC/FIS/68609/2006 and PEst-OE/MAT/UI0219/2011) and by Philips Lighting.

- ¹A. Anders, H. Schneidenbach, and D. Sunder, *IEEE Trans. Plasma Sci.* **19**, 324 (1991).
- ²F. Schuda, *Cermax Lamp Engineering Guide* (Perkin Elmer Optoelectronics, Sunnyvale, CA, 1998).
- ³U. Krönert, M. Stucky, and S. Müller, *Untersuchung der Auswirkung des Bogenansatzes auf die elektromagnetische Emission (EME)*. BMBF Report 13N7110/2 (Fachhochschule Kaiserslautern, Kaiserslautern, Germany, 2000).
- ⁴O. Minayeva and D. Doughty, *Bull. Am. Phys. Soc.* **52**, 44 (2007). Available at: <http://meetings.aps.org/link/BAPS.2007.GEC.MWP1.38>
- ⁵U. Hechtfisher, *J. Appl. Phys.* **110**, 073309 (2011).
- ⁶E. P. Velikhov, A. S. Kovalev, and A. T. Rakhimov, *Physical Phenomena in a Gas Discharge Plasma* (Nauka, Moscow, 1987), in Russian.
- ⁷F. G. Baksht, A. A. Kostin, N. K. Mitrofanov, and S. M. Shkol'nik, in *Proc. Conf. on Physics of Low-Temperature Plasma, Petrozavodsk, Russia, June 1995* (PGU, Petrozavodsk, RF, 1995), pp. 191-193, in Russian.
- ⁸F. G. Baksht, G. A. Dyuzhev, N. K. Mitrofanov, and S. M. Shkol'nik, *Tech. Phys.* **42**, 35 (1997).
- ⁹S. M. Shkol'nik, in *Encyclopaedia of Low-Temperature Plasmas*, vol. 2, edited by V. E. Fortov (Nauka, Moscow, 2000), pp. 147-165, in Russian.
- ¹⁰G. Yang and J. Heberlein, *Plasma Sources Sci. Technol.* **16**, 529 (2007).
- ¹¹G. Yang and J. Heberlein, *Plasma Sources Sci. Technol.* **16**, 765 (2007).
- ¹²J. Heberlein, J. Mentel, and E. Pfender, *J. Phys. D: Appl. Phys.* **43**, 023001 (2010).
- ¹³S. M. Shkol'nik, *Plasma Sources Sci. Technol.* **20**, 013001 (2011).
- ¹⁴M. Mitchner and C. H. Kruger, *Partially Ionized Gases* (Wiley, New York, 1973).
- ¹⁵Yu. P. Raizer, *Gas Discharge Physics* (Springer, Berlin, 1991).
- ¹⁶N. A. Almeida, M. S. Benilov, U. Hechtfisher, and G. V. Naidis, *J. Phys. D: Appl. Phys.* **42**, 045210 (2009).
- ¹⁷M. S. Benilov, *J. Phys. D: Appl. Phys.* **41**, 144001 (2008).
- ¹⁸N. A. Almeida, M. S. Benilov, and G. V. Naidis, *J. Phys. D: Appl. Phys.* **41**, 245201 (2008).
- ¹⁹M. S. Benilov, *J. Phys. D: Appl. Phys.* **40**, 1376 (2007).
- ²⁰M. S. Benilov and M. J. Faria, *J. Phys. D: Appl. Phys.* **40**, 5083 (2007).
- ²¹J. Mentel and J. Heberlein, *J. Phys. D: Appl. Phys.* **43**, 023002 (2010).